Molecular Cell, Vol. 12, 863–874, October, 2003, Copyright ©2003 by Cell Press

Structural Basis for Arl1-Dependent Targeting of Homodimeric GRIP Domains to the Golgi Apparatus

Bojana Panic,[1] Olga Perisic,[1] Dmitry B. Veprintsev,[2] Roger L. Williams,[1] and Sean Munro[1,*]
[1]MRC Laboratory of Molecular Biology
[2]Centre for Protein Engineering
MRC Centre
Hills Road
Cambridge CB2 2QH
United Kingdom

Summary

Golgins are large coiled-coil proteins that play a role in Golgi structure and vesicle traffic. The Arf-like GTPase Arl1 regulates the translocation of GRIP domain-containing golgins to Golgi membranes. We report here the 1.7 Å resolution structure of human Arl1-GTP in a complex with the GRIP domain of golgin-245. The structure reveals that the GRIP domain consists of an S-shaped arrangement of three helices. The domain forms a homodimer that binds two Arl1-GTPs using two helices from each monomer. The structure is consistent with golgin-245 forming parallel coiled-coils and suggests how Arl1-GTP/GRIP complexes interact with Golgi membranes via the N termini of Arl1-GTP and the C-terminal tails of the GRIP domains. In cells, bivalent association with Arl1-GTP would increase residence time of the golgins on Golgi membranes. Despite no conservation of sequence, topology, or even helical direction, several other effectors form similar interactions with small GTPases via a pair of α helices, suggesting a common structural basis for effector recognition.

Introduction

Small GTPases of the Ras superfamily control a wide range of cellular events and are divided into the Ras, Rho, Ran, Rab, and Arf classes (Takai et al., 2001). For all classes, a cycle of GTP binding and hydrolysis is linked to a conformational change which alters interaction with effectors (Vetter and Wittinghofer, 2001). The Arf class of GTPases is distinguished from the others by an N-terminal amphipathic helix, typically myristoylated, that mediates interaction with membranes (Chavrier and Goud, 1999). In addition, the Arf GTPases undergo a "front-back" change so that in the GTP-bound form the amphipathic helix is displaced from a hydrophobic pocket in the GTPase and instead acts to stabilize interaction with lipid bilayers (Antonny et al., 1997; Pasqualato et al., 2002). Genetic and biochemical evidence has shown that Arf GTPases play central roles in both membrane traffic and cytoskeletal organization. Activation of Arf GTPases is usually controlled by exchange factors resident on specific organelles, with the GTP-bound GTPase then recruiting specific effectors to that organelle (Donaldson and Jackson, 2000). For example, Arf1 recruits COP I vesicle coats to Golgi membranes, and the distantly related Sar1 recruits COP II coats to the endoplasmic reticulum (ER). Arf1 also binds directly to the Golgi-localized protein GGA1, an adaptor that recruits cargo into Golgi-derived clathrin-coated vesicles. Arf1 has a number of close relatives, including the plasma membrane-localized Arf6 that modulates the actin cytoskeleton and endocytosis via generation of PtdIns(4,5)P_2 (Krauss et al., 2003; Niedergang et al., 2003). Beyond this, there is a large number of more distantly related proteins known as Arf-like (Arl) GTPases that share structural features with Arf1 and Sar1, but whose functions are less well understood (Clark et al., 1993; Pasqualato et al., 2002).

There are at least ten Arls in humans which all share with the Arfs an N-terminal amphipathic helix and, in most cases, a consensus sequence for N-myristoylation (Antonny et al., 1997; Pasqualato et al., 2002). The function of most Arl proteins is unclear, but their importance is suggested by the observations that mutation of Arl1 in *Drosophila* is zygotically lethal (Tamkun et al., 1991) and that deletion in mice of Arf-related protein (ARFRP1 or ARP) causes embryonic lethality (Mueller et al., 2002). Arl2 has been implicated in tubulin assembly and microtubule polymerization, but its effector in this process is not known (Bhamidipati et al., 2000). In addition, Arl2-GTP binds to the phosphodiesterase (PDE) δ subunit, which has been proposed to act as a transport factor for the PDE catalytic subunits, and other prenylated proteins including GTPases (Hanzal-Bayer et al., 2002).

Of the other Arls, perhaps the best understood is Arl1, which localized to the Golgi apparatus of both mammalian cells and yeast (Lowe et al., 1996; Gangi Setty et al., 2003). Arl1 is myristoylated, and mutation of the N-terminal myristoylation site abrogates Golgi targeting (Lee et al., 1997; Lu et al., 2001). Yeast two-hybrid screens for potential effectors of human Ar1l identified two Golgi-localized proteins, golgin-97 and golgin-245 (also termed p230) (Fritzler et al., 1995; Erlich et al., 1996; Lu et al., 2001; Van Valkenburgh et al., 2001). These are two members of a set of large coiled-coil proteins that have been found on the Golgi apparatus and which are often referred to as "golgins." The golgins have been implicated in Golgi formation and maintenance as well as in vesicular transport. Golgin-97 and golgin-245, along with GCC88 and GCC185, are peripheral membrane proteins that share a C-terminal GRIP domain. This ~50 residue domain is both necessary and sufficient for targeting to the Golgi apparatus and is conserved in animals, fungi, plants, and protozoa (Barr, 1999; Kjer-Nielsen et al., 1999a; Munro and Nichols, 1999; McConville et al., 2002). Arl1 is required for targeting GRIP domain proteins to the Golgi apparatus in both yeast and mammalian cells and has been shown to bind directly to the GRIP domain in a GTP-dependent manner (Gangi Setty et al., 2003; Panic et al., 2003). Arl1 appears to be predominantly localized to Golgi membranes, and relocation of Arl1-GTP to a different organ-

*Correspondence: sean@mrc-lmb.cam.ac.uk

elle causes relocation of a GRIP golgin (Lu and Hong, 2003).

Although the precise function of the GRIP golgins is still unclear, golgins such as p115 and GM130 have been shown to participate in both tethering of transport vesicles to Golgi membranes prior to fusion and in stacking cisternae to create the higher order structure of the Golgi (Pfeffer, 1999; Shorter and Warren, 2002; Barr and Short, 2003; Gillingham and Munro, 2003). In yeast, deletion of either Arl1p or Imh1p, the only GRIP domain protein, results in missorting of vacuolar proteins and, in much more severe growth phenotypes when combined with loss of Ypt6p, another GTPase that acts in this process (Li and Warner, 1996; Tsukada et al., 1999; Bonangelino et al., 2002). Such phenotypes would be consistent with a role in tethering vesicles returning from endosomes back to the *trans* Golgi. It seems likely that both vesicle tethering and cisternal stacking roles will require that the golgins are accurately targeted to specific parts of the Golgi apparatus. Golgin-245 is found on the *trans* face of the Golgi apparatus (Kooy et al., 1992), and the GRIP domains of all four human GRIP domain golgins are sufficient to confer this compartment-specific targeting (Luke et al., 2003).

In this paper, we report a 1.7 Å resolution X-ray structure of a complex between a human GRIP domain and GTP-bound Arl1. The structure reveals that the GRIP domain is a dimer, allowing two Arl1 proteins to interact simultaneously with a golgin. To our knowledge, such a dyad-symmetrical interaction of a small GTPase with an effector has not been described previously. The interaction interface between Arl1 and the GRIP domain shares features with those formed between several other Ras-like GTPases and their effectors, despite a range of effector topologies. The specificity of the interactions is dictated by packing restraints at the interface with the GTPase.

Results and Discussion

Preparation and Crystallization of an Arl1-GTP/GRIP Domain Complex

The GRIP domain was initially defined on the basis of related sequences present at the C termini of several Golgi coiled-coil proteins (Barr, 1999; Kjer-Nielsen et al., 1999a; Munro and Nichols, 1999). There are four GRIP domain-containing proteins in humans and *Drosophila*, and one in fungi and plants (Figure 1A). Direct binding has previously been reported between recombinant forms of the GRIP domain of *S. cerevisiae* Imh1p and Arl1p-GTP. It has also been reported that human Arl1p interacts with golgin-245 and golgin-97 in a yeast two-hybrid assay (Lu et al., 2001; Van Valkenburgh et al., 2001). *E. coli*-expressed forms of all four human GRIP domains bind directly to human Arl1 in a GTP-dependent fashion (Figure 1B), suggesting that GRIP domains defined by sequence may all share the capacity to bind to Arl1p-GTP.

The C-terminal 59 residues of human golgin-245 encompassing the GRIP domain was coexpressed in *E. coli* with human Arl1 lacking the N-terminal 14 residues. This N-terminal region is very likely to form an amphipathic helix, as such a helix has been observed in the structures of the GDP-bound forms of all Arf family members so far examined, including that of yeast Arl1p (Amor et al., 2001). This helix is displaced in the GTP-bound forms of other Arf family GTPases to expose the hydrophobic face for association with membranes, and its removal was necessary for crystallization of GTP-bound forms of Arf1p and Sar1p (Bi et al., 2002; Shiba et al., 2003). The GTPase active site mutant Q71L was incorporated into Arl1 to ensure that the protein accumulated in the GTP-bound form. Complexes were purified by affinity chromatography and gel filtration in the presence of Mg^{2+} and GTP.

Overall Structure of the Arl1-GTP/GRIP Domain Complex

The complex of the human golgin-245 GRIP domain with human Arl1(Q71L) crystallized in space group $P2_1$ with unit cell dimensions a = 72.5, b = 89.7, c = 72.5, β = 110.7. There are four Arl1(Q71L)-GTP/GRIP domain complexes in the asymmetric unit. The structure was solved using Se-Met multiple anomalous dispersion (MAD) data (Table 1). There are only minor differences in conformation among the four Arl1/GRIP complexes in the asymmetric unit.

The structure reveals that the GRIP domain forms a homodimer, with each GRIP domain bound to an Arl1-GTP (Figure 2). The resulting dyad symmetric arrangement of the Arl1 proteins leaves their N termini facing the same direction so that the two N-terminal amphipathic helices absent from the structure would be able to interact simultaneously with a lipid bilayer. The overall extent of the residues in the GRIP domain that participate in dimerization or Arl1 binding corresponds well to the 40–50 residue region conserved among different GRIP domains, and specifically to the 45 residue portion of golgin-245 that is sufficient for some Golgi targeting (gray bar in Figure 1C; Kjer-Nielsen et al., 1999b). Previous mutagenesis studies have also identified a number of residues in the GRIP domain that are required for Golgi targeting (summarized in Figure 1C). In a previous structural analysis of yeast Arl1p-GDP in the absence of the GRIP domain, the protein formed an intermolecular disulfide bond in the crystal via Cys 80, although this bond is unlikely to occur in the reducing environment of the cytoplasm (Amor et al., 2001). In the Arl1-GTP/GRIP crystal, this cysteine residue is buried in the Arl1/GRIP interface (see below), which has prevented such artifactual disulfide bond formation.

Structure of Arl1(Q71L)-GTP

Like other Arf family GTPases, the GTP-bound Arl1 (Q71L) overall fold consists of six β strands surrounded by five α helices (Figure 2). Comparison of the human Arl1(Q71L)-GTP with the previously reported yeast Arl1-GDP (Amor et al., 2001), shows that the region from 40 to 82 changes conformation upon GTP binding. This is consistent with other members of the Arf family GTPases (Goldberg, 1998; Pasqualato et al., 2001). The region from 51 to 67 (strands β2 and β3) has been referred to as the "interswitch" region (Pasqualato et al., 2002) and is located between switch 1 (residues 40–50) and switch 2 (residues 68–82). In the GTP-bound form of Arl1, the interswitch region has moved two residues with respect

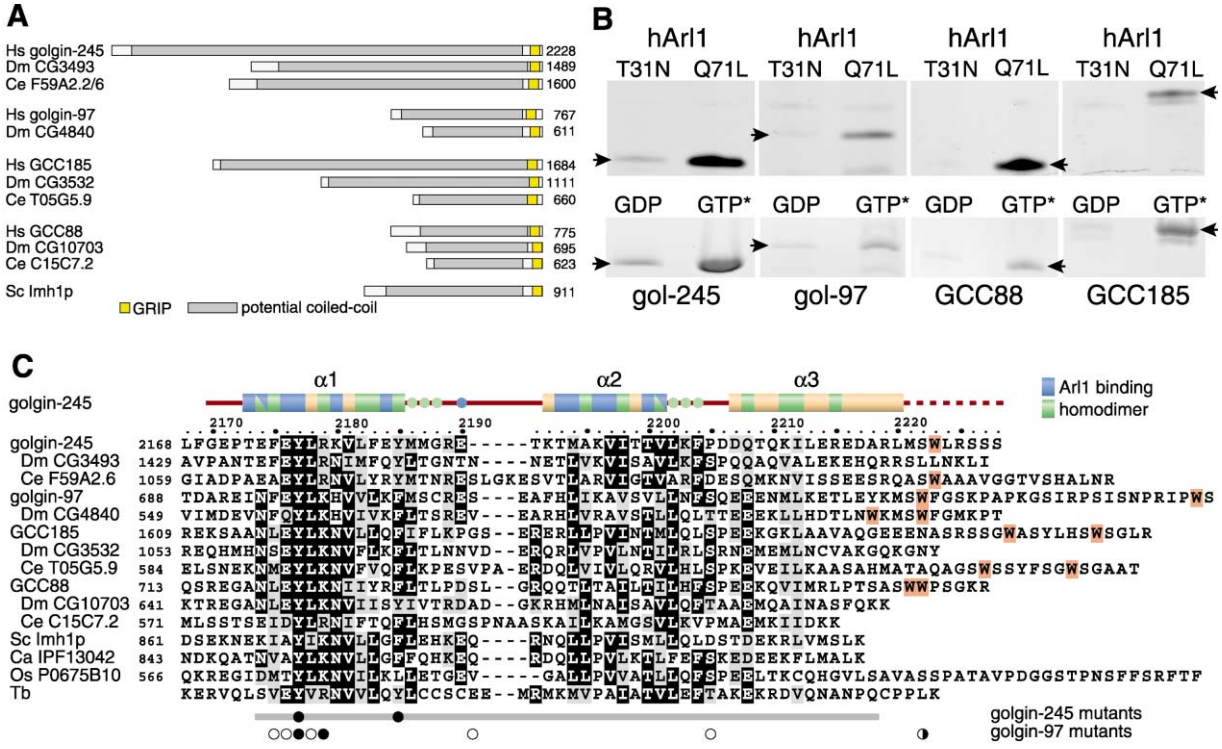

Figure 1. Domain Structure and Sequence Alignment of GRIP Domain-Containing Proteins

(A) Schematic representation of the four human GRIP domain proteins, and their homologs in *Drosophila melanogaster* (Dm) and *Caenorhabditis elegans* (Ce). Also shown is Imh1p, the single GRIP domain protein of *Saccharomyces cerevisiae* (Sc). Sequence homology suggests that the gene encoding the *C. elegans* homolog of golgin-245 probably comprises two adjacent predicted genes in the genome (F59A2.2 and F59A2.6). There is a fifth protein in the human genome that ends with a GRIP domain, Ran binding protein 2α (RanBP2α), but it appears to be the product of a recent fusion of duplications of the genes for RanBP2 and GCC185, and its significance is unclear.

(B) Binding of the GRIP domains from the indicated human golgins to Arl1. Extracts of *E. coli* expressing the His_6-tagged GRIP domains of golgin-245, golgin-97, GCC88, and GCC185 (C-terminal 58, 78, 62, and 110 residues, respectively) were applied to glutathione beads loaded with either human GST-Arl1 with mutations to lock it in the GDP (T31N) or GTP (Q71L) bound forms (upper panels), or GST-Arl1 loaded with GDP or the nonhydrolysable analog GMPPNP (GTP*) as described previously (lower panels) (Panic et al., 2003). After washing, bound proteins were eluted with SDS sample buffer and analyzed by gel electrophoresis and Coomassie blue staining.

(C) Alignment of the C termini of the indicated human GRIP domain proteins and their homologs in other species. Sequences were aligned with Clustal W, and residues identical, or related, in seven or more of the sequences are indicated by black or gray, respectively (BoxShade), and tryptophans are marked in orange. A schematic of the structure of the golgin-245 GRIP domain is shown above the alignment with the interacting residues marked as indicated. The residue numbering for golgin-245 is based on that of Swissprot accession Q13439 (isoform 4) (Erlich et al., 1996). Residues in the GRIP domains of golgin-245 or golgin-97 that have been mutated in previous studies are indicated with circles (filled, loss of Golgi targeting; open, normal targeting; half filled, reduced targeting) (Barr, 1999; Kjer-Nielsen et al., 1999a; Munro and Nichols, 1999; Lu and Hong, 2003). The gray bar indicates the minimal portion of golgin-245 that shows some Golgi targeting (Kjer-Nielsen et al., 1999b). Species as in (A), or *Candida albicans* (Ca), *Oryza sativa* (Os), and *Trypanosoma brucei* (Tb).

to the rest of the β sheet. This register shift is characteristic of the Arf family GTPases and has the effect of communicating conformational changes in the switch regions with the other side of the molecule so that the N-terminal amphipathic helix swings away from the body of the GTPase upon GTP binding (Hanzal-Bayer et al., 2002; Pasqualato et al., 2002).

In Arl1-GTP, switch 1 has a conformation that enables Thr 48 to act as a ligand of the nucleotide-associated Mg^{2+}. GTP binding also results in a conformational change of switch 2, enabling the 67-DXXG-70 motif to coordinate the γ-phosphate of the GTP. These conformational changes are characteristic of nucleotide-dependent structural rearrangements in the Ras superfamily of GTPases (Vetter and Wittinghofer, 2001). While the overall fold of the Arl1(Q71L) is similar to the GTP-bound forms of Arf1 and Arl2, there are local surface features in the switch/interswitch regions that can account for the specificity of the Arl1-GTP/GRIP interaction (see below).

GRIP Domain Dimerization

The GRIP domain consists of three antiparallel α helices arranged in an S-shaped configuration (Figures 2 and 3). The surface of the S-shaped domain is slightly curved, and the convex face interacts with the Arl1 while the concave face pairs with another GRIP domain in a parallel α-helical "handshake." The interaction between GRIP domains in the crystal is extensive (2282 $Å^2$ of solvent-accessible area is buried) and overwhelmingly hydrophobic, with only a single intermolecular hydrogen bond (Arg 2179 to carbonyl oxygen of Leu 2202; Figure 3A). The extensive interface between the GRIP domains suggests that this homodimeric interaction is probably

Table 1. Data Collection, Structure Determination, and Refinement Statistics

Data collection and MAD phasing statistics			
Data Set	Peak[c]	Inflection[c]	Remote[c]
Resolution	1.7 Å	1.9 Å	1.9 Å
Completeness (last shell)	98.7 (92.3)	100.0 (98.8)	99.9 (100.0)
R_{merge}[a]	0.062	0.057	0.065
Redundancy	3.6	3.7	3.7
$<I/\sigma>$ (last shell)	13.9 (1)	16.6 (2.5)	11.7 (1.5)
Phasing statistics			
Phasing power (iso)[b]	—	0.78	1.1
Phasing power (anom)[b]	1.48	1.42	1.2
Se sites found/expected	39/48		
FOM after SHARP	0.43		
FOM after SOLOMON	0.79		
Refinement statistics			
Resolution	67–1.7 Å		
Protein atoms	7148		
Waters	266		
R_{cryst}[d]	0.22		
R_{free}[d] (% data used)	0.25 (3.4)		
Rmsd from ideality[e]			
Bonds	0.014 Å		
Angles	1.5°		
Dihedrals	6.0°		

[a] $R_{merge} = \Sigma_{hkl}\Sigma_i|I_i(hkl) - <I(hkl)>|/\Sigma_{hkl}\Sigma_i I_i(hkl)$.
[b] The phasing power is defined as the ratio of the r.m.s. value of the heavy atom structure factor amplitudes to the r.m.s. value of the lack-of-closure error.
[c] Data sets were collected at ESRF beamline ID14-4 at 12.6612, 12.6590, and 13.2 keV for the peak, inflection, and remote data sets, respectively.
[d] R_{cryst} and $R_{free} = \Sigma|F_{obs} - F_{calc}|/\Sigma F_{obs}$; R_{free} calculated with the percentage of the data shown in parentheses.
[e] Rms deviations for bond angles and lengths in regard to Engh and Huber parameters.

present in solution, and this was confirmed in two ways. First, versions of the GRIP domain were expressed in *E. coli* with either His_6 or MBP tags. The MBP form could be precipitated with Ni^{2+}-NTA-agarose only if it was coexpressed with the His_6-tagged species, or mixed with it after lysis (Figure 3B). Second, when the GRIP domain was subjected to equilibrium centrifugation, monomers and dimers were found to be in equilibrium in solution, with the sedimentation profile indicating a K_d for dimerization of about 2.5 μM (Figure 3C).

Examination of the dimer interface shows that helix α1 of the GRIP domain has a pivotal role. This helix has a hydrophobic face consisting of residues Phe 2175, Leu 2178, Leu 2182, and Tyr 2185 that lines up along the dyad axis and primarily interacts with helices α2 and α3 and connecting loops from the other half of the dimer (Figure 3A). Many of the residues that comprise the interface are well conserved in evolution, with Phe or Tyr equivalent to Tyr 2185 of golgin-245 present in almost all GRIP domains (Figure 1C). This residue, near the C-terminal end of helix α1, makes hydrophobic contacts with Tyr 2185 and Met 2186 from the dyad-related monomer. The importance of these interactions is underscored by mutations in two conserved residues in helix α1 having been previously reported to result in loss of Golgi targeting of GRIP domains (Barr, 1999; Kjer-Nielsen et al., 1999a). These mutations are Y2185A in golgin-245 and K699A in golgin-97 (equivalent to Arg 2179 in golgin-245, which forms extensive hydrophobic contacts as well as an intermolecular hydrogen bond).

Interaction between Arl1-GTP and the GRIP Domain

All of the contacts that the GRIP domain makes with Arl1 are via GRIP helices α1 and α2, with α1 forming most of the switch 1 interactions and α2 forming most of the switch 2 interactions (Figure 4). Interaction with the Arl1 switch/interswitch regions in the crystal structure provides a rational explanation for the GTP-dependent binding of the GRIP domain seen in vitro and in vivo. The only residue in the GRIP domain that interacts with both switch 1 and switch 2 is the very well conserved Tyr 2177. Mutation of this residue to alanine in golgin-245 and several other GRIP domains has been shown to result in loss of Golgi targeting in mammals, yeast, and protozoa (Kjer-Nielsen et al., 1999a; Munro and Nichols, 1999; McConville et al., 2002). Moreover, the same residue is required for Arl1 binding by the GRIP domain of the yeast protein Imh1p and for yeast two-hybrid interaction between the GRIP domain of golgin-245 and human Arl1 (Van Valkenburgh et al., 2001; Panic et al., 2003). Tyr 2177 protrudes into a pocket on the surface of the Arl1 that is lined by a cluster of hydrophobic residues from the interswitch and switch 2 (Phe 51, Leu 66, Ile 74, Tyr 77, and Tyr 81; Figure 4). This "selectivity pocket" appears to be one important determinant of the specificity of the Arl1-GTP/GRIP interaction. At the bottom of this selectivity pocket, the OH of Tyr 2177 forms a hydrogen bond with the OH of Tyr 81 in switch 2. Although a tyrosine at the position equivalent to Tyr 2177 is conserved in all GRIP domains, mutagenesis indicates that the hydrogen bond formed with Tyr 81 is

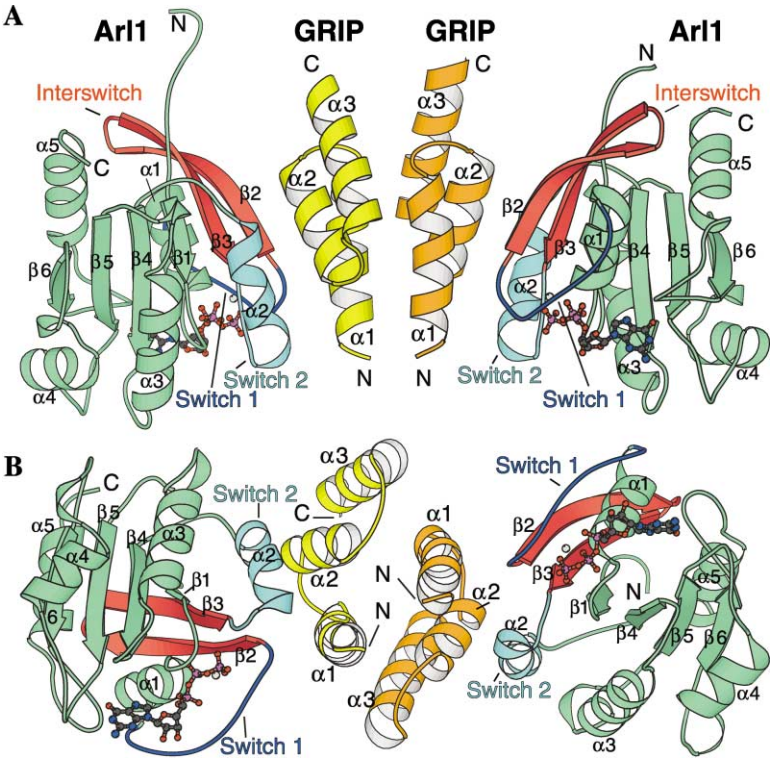

Figure 2. Structure of the Human Arl1/Golgin-245 GRIP Domain Complex

(A) Ribbon diagram of the Arl1(Q71L)-GTP/Mg^{2+}/GRIP domain complex. The golgin-245 GRIP domain forms a homodimer (one GRIP molecule is colored yellow, the other orange), with each GRIP domain binding one Arl1 molecule. Arl1 is shown in green, with switch 1 residues highlighted in blue, switch 2 residues in cyan, and interswitch in red. The GTP is shown as balls-and-sticks with Mg^{2+} as a gray sphere.

(B) A view of Arl1/GRIP complex approximately perpendicular to the view shown in (A).

not essential, as substitution of Tyr 2177 with Phe did not significantly affect Golgi localization (Kjer-Nielsen et al., 1999a). This suggests that the hydrophobic interactions of the Tyr 2177 with the selectivity pocket are paramount for Arl1-GTP/GRIP binding. In the GDP complexes of both Arls and Arfs, the selectivity pocket is occupied by the phenylalanine at residue 51 in Arl1 or its equivalent. This, and other structural changes in the switch regions, presumably prevents binding of the GRIP domain to Arl1-GDP.

Selectivity of the Golgin GRIP Domains for Arl1-GTP

The golgin-245 GRIP domain binds selectively to Arl1-GTP and not to other Arf-family GTPases such as Arfs1-6 and Arl2 (Van Valkenburgh et al., 2001; Lu and Hong, 2003). Comparison of the Arl1-GTP/GRIP structure with that of Arf1-GTP (Shiba et al., 2003) shows that the switch 2 region involved in effector binding may account for much of the effector selectivity. In particular, a hydrophobic selectivity pocket on Arl1 wide enough to accommodate GRIP Tyr 2177 appears to be a unique feature of Arl1. In Arf1, the residues lining the selectivity pocket are identical to those of Arl1 except for Leu 77 of Arf1, corresponding to Tyr 77 in Arl1. In Arf1, Leu 77 fills in much of the selectivity pocket because the two δ methyl groups of the leucine protrude into the pocket due to sp^3 hybridization at the γ carbon, whereas the sp^2 hybridization at the γ-carbon of the tyrosine in Arl1 creates more space in the pocket. All of the Arf family GTPases have a Leu at residue 77, whereas only Arl1, Arl2, and Arl3 have a tyrosine at this position (Figure 4B). Although Arl2 has this tyrosine, the opposite corner of the selectivity pocket in Arl2 is partially filled in by a leucine (residue 73 of Arl2, corresponding to Ile 74 of Arl1), presumably cramping entry of the critical GRIP Tyr 2177. Other residues in the interface are likely to contribute to selectivity for Ar1l-GTP. For example, Arl1 Cys 80 makes a hydrogen bond to GRIP Thr 2200 and is well conserved in Arl1 from different species (Figure 4C). In contrast, a histidine is conserved at this position in the Arf proteins, and a C80H mutation in Arl1 eliminates a yeast two-hybrid interaction with the golgin-245 GRIP domain (Lu and Hong, 2003), presumably because of the steric effects of the bulkier histidine residue.

Just as comparison of Arl1-GTP with Arf1-GTP suggests differences that could account for effector selectivity, comparison of the GRIP domain with the Arf1 effector domain N-GAT shows differences that could account for GTPase selectivity. The presence of a GRIP tyrosine (Tyr 2177) that occupies the selectivity pocket appears to be a unique GRIP domain feature. Although a variety of folds have been observed for various Arf and Arl effectors, in all cases except for the GRIP domains either an isoleucine or leucine from the effector occupies the selectivity pocket of the GTPase. For example, Ile 197 in the N-GAT domain occupies a position in space analogous to Tyr 2177 of golgin-245 GRIP, but the N-GAT isoleucine makes a shallower contact with Arf1 (Shiba et al., 2003).

The only other structure of an Arl/effector complex that has been reported is that of Arl2 with PDEδ (Hanzal-Bayer et al., 2002). In this complex, the effector makes extensive interactions with switch 1 of the Arl2 (849 $Å^2$ buried in the switch 1/PDEδ interface) and forms an intermolecular β sheet similar to Ras/effector complexes (Nassar et al., 1995; Pacold et al., 2000). The PDEδ effector domain makes only limited contacts with switch 2 (338 $Å^2$ buried in the switch 2/PDEδ interface).

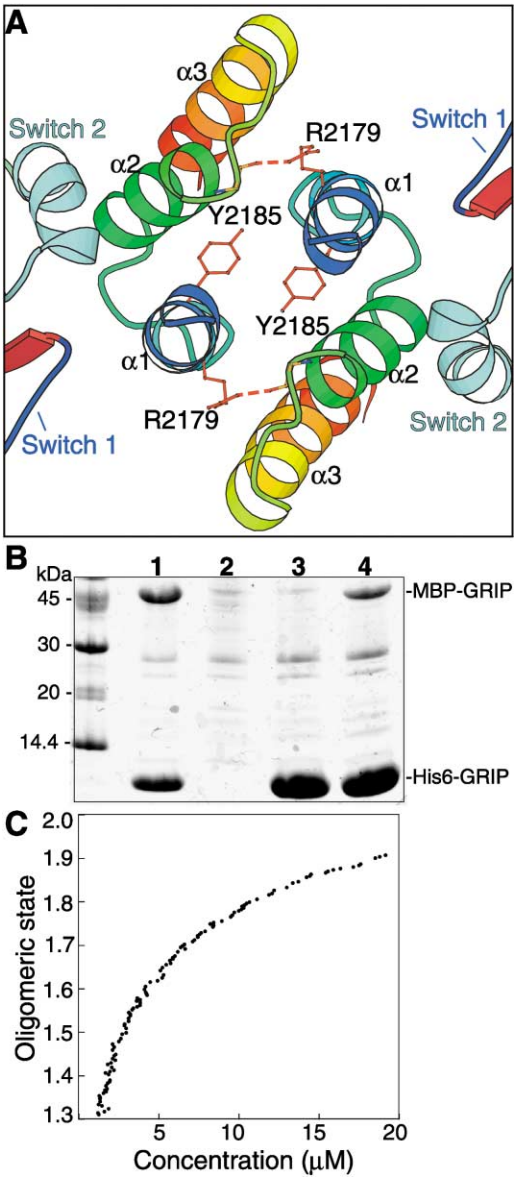

Figure 3. The Golgin-245 GRIP Domain Homodimerizes in the Crystal and in Solution

(A) GRIP homodimer interface. Each GRIP domain from a dyad-symmetric homodimer is colored in rainbow colors, from blue (N terminus) to red (C terminus). Two residues from the homodimer interface are highlighted: Tyr 2185, which forms a hydrophobic interaction, and Arg 2179, which makes a hydrogen bond to the carbonyl oxygen of Leu 2202. Mutation of either of these residues results in loss of Golgi targeting (Kjer-Nielsen et al., 1999a; Lu and Hong, 2003).

(B) GRIP domain homodimerization as shown by coprecipitation of His_6-tagged and MBP-tagged GRIP domains. Cytosol from *E. coli* coexpressing the two proteins from a single polycistronic plasmid (lane 1), expressing only MBP-GRIP (lane 2), expressing only His_6-GRIP (lane 3), or a mixture of cytosols expressing the two proteins individually (lane 4) was bound to Ni-NTA beads. Imidazole eluates were analyzed by SDS gel electrophoresis and Coomassie staining.

(C) The oligomerization state of the His_6-GRIP domain derived by analytical ultracentrifugation is best described by a monomer-dimer equilibrium with a $K_d = 2.5 \pm 0.9$ μM. The results are presented as a plot of the observed oligomerization state (i.e., the apparent molecular weight divided by the molecular weight of the GRIP monomer) as a function of protein concentration.

In contrast, the GRIP domain makes a much more extensive interface with switch 2 than with switch 1 (730 Å^2 buried in the switch 2/GRIP interface versus 308 Å^2 for the switch 1 interface out of a total of 1329 Å^2 buried in the Arl1/GRIP interface).

A Shared Mode of GTPase-Effector Recognition

Several effector domains of Ras superfamily GTPases are helical, including N-GAT domains, Arfaptin2, the protein kinase N (PKN) ACC finger, and from this work, GRIP domains (Maesaki et al., 1999; Tarricone et al., 2001; Collins et al., 2003; Shiba et al., 2003). Structural comparison of the complexes between these effectors and their GTPases shows a shared mode of interaction. For each of the effectors, antiparallel helices contact hydrophobic patches formed by switch/interswitch regions of the GTPase (Figure 5). Because the vast majority of the interactions are with residues in the effector helices and not in the connecting loops, and because the interactions are principally nondirectional hydrophobic interactions between side chains, there are no constraints on the connecting topology or even the direction of the effector helices. Thus, the direction of the equivalent helices is swapped N- to C terminus in N-GAT and Arfaptin2 relative to GRIP, and the connection between the two helices is swapped from one end of the helices to the other in N-GAT relative to Arfaptin2 (Figure 5B). A more distant variant is the complex between Rab3A and rabphilin-3A, where the effector lacks one of the two helices, and instead a short motif in rabphilin-3A makes additional contacts outside of the Rab3A switch regions (Ostermeier and Brunger, 1999). This plastic mode of interaction of these helical effectors with their GTPases leads to a striking structural mimicry that was completely unsuspected from sequence alignments.

The C-Terminal Tail of the GRIP Domain

Although the GRIP domain is located near the C terminus of all proteins in which it has been found, in many cases the domain is followed by an extension of typically 5–30 residues before the end of the protein. Despite being heterogeneous in length and sequence, and indeed not present in all GRIP domain proteins, there are indications that these C-terminal tails may be functionally important. First, some of the tails have shared sequence features, most notably one or two tryptophan residues, which in some cases are interspersed with additional bulky hydrophobic residues (Figure 1C). Second, Golgi targeting of the golgin-97 GRIP domain was reported to be reduced when the tryptophan in the tail (Trp 744) was mutated to alanine (Barr, 1999). Human golgin-245 occurs in two splice isoforms that differ only in these tail residues (Erlich et al., 1996). In the isoform used for these studies, the C-terminal seven residues are SWLRSSS, but inclusion of an extra exon results in these being replaced with FTSPRSGIF, with the latter version being represented by 3 of the 20 ESTs for human golgin-245 in the current GenBank database. The significance of this is unclear, as Golgi targeting of the two forms was apparently indistinguishable (Kjer-Nielsen et al., 1999b), but similar alternative splicing is seen in ESTs from mice and rats, suggesting that it has been conserved at least through recent evolution. As with golgin-97, mutation

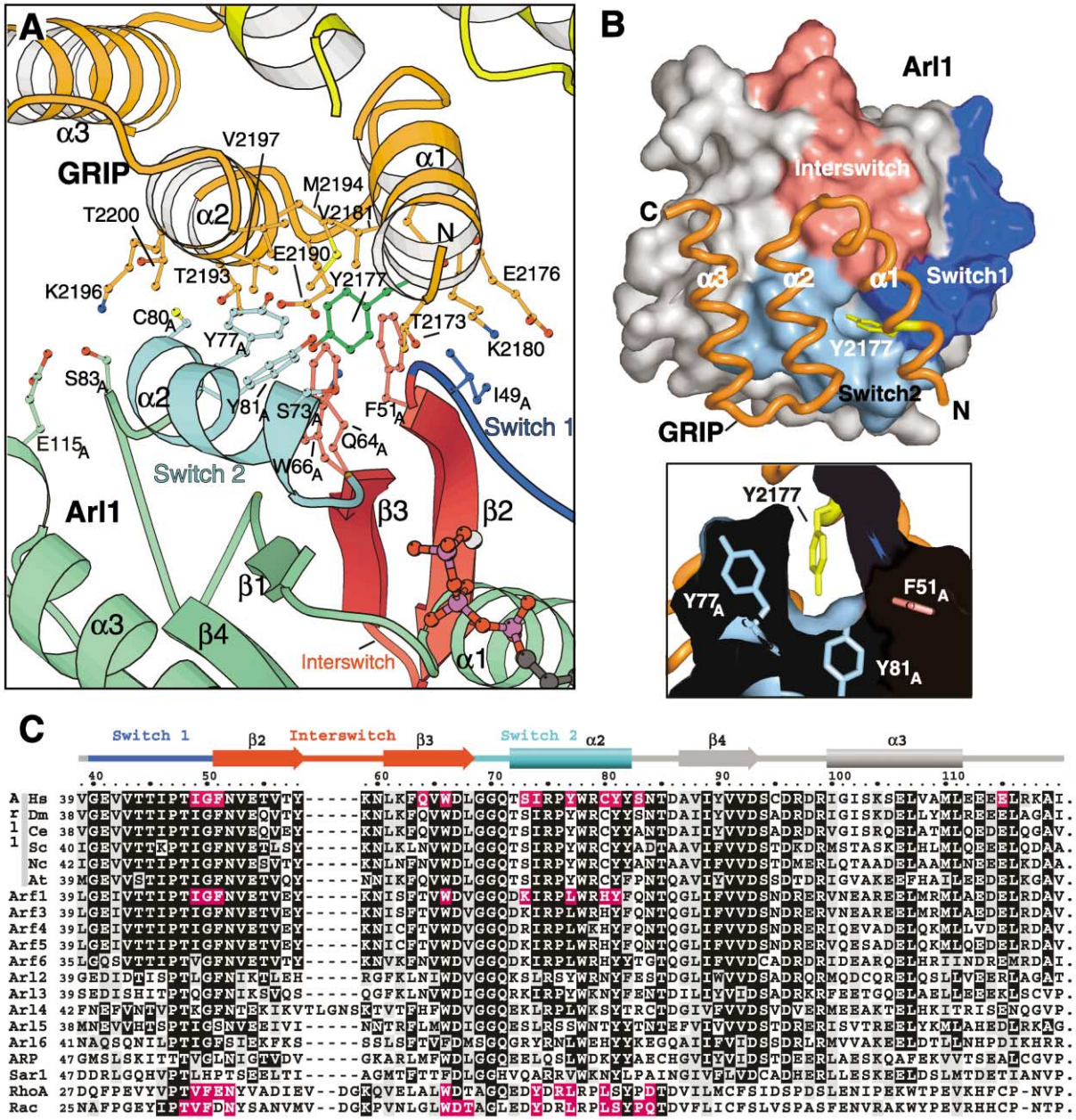

Figure 4. The Arl1-GTP/GRIP Interface

(A) GRIP domain helices α1 and α2 are positioned against the switch 1 and switch 2 regions of Arl1. The side chains of the Arl1 and GRIP residues involved in the interaction are shown as balls-and-sticks. The GRIP domain residues are orange, with the conserved Tyr 2177 in green. The Arl1 switch 1 residues are shown in blue, switch 2 residues in cyan, interswitch in red, and the rest of Arl1 in light green.

(B) Tyr 2177, a residue that is strictly conserved among GRIP domains, slots into the Arl1 hydrophobic selectivity pocket. In the upper panel, the Arl1 molecular surface is colored gray, with switch and interswitch regions colored as in (A). The backbone of the GRIP monomer is shown as an orange worm, with the side chain of Tyr 2177 in yellow. In the lower panel, a cut through the Arl1 surface shows a view from the bottom of the selectivity pocket and highlights three of the Arl1 residues lining the pocket.

(C) Alignment of the switch region of Arl1 from various species, and those of the indicated human small GTPases. Residues identical or related in ten or more of the sequences are shaded black or gray, respectively. Species are as in Figure 1, or *Neurospora crassa* (Nc) and *Arabidopsis thaliana* (At). The structure of Arl1 in the Arl1-GTP/GRIP crystal is shown schematically, and the residues in Arl1 that interact with the GRIP domain are shaded in purple. The effector binding residues in Arf1, RhoA, and Rac are also boxed in purple, based on the structures of Arf1/N-GAT, RhoA/PKN (contact 2), and Rac/Arfaptin2 (Maesaki et al., 1999; Tarricone et al., 2001; Shiba et al., 2003).

of Trp 2223 did not prevent the Golgi targeting of the SWLRSSS form of the GRIP domain, but reduced the Golgi-specific signal (Figure 6A). Moreover, photobleaching of the cytoplasmic pool of GFP-GRIP revealed that the W2223A mutation reduced the half-time for exchange between the Golgi and cytoplasmic pools from ~35 s to ~13 s (Figure 6B). This is also consistent with the observation that Golgi targeting of the golgin-245

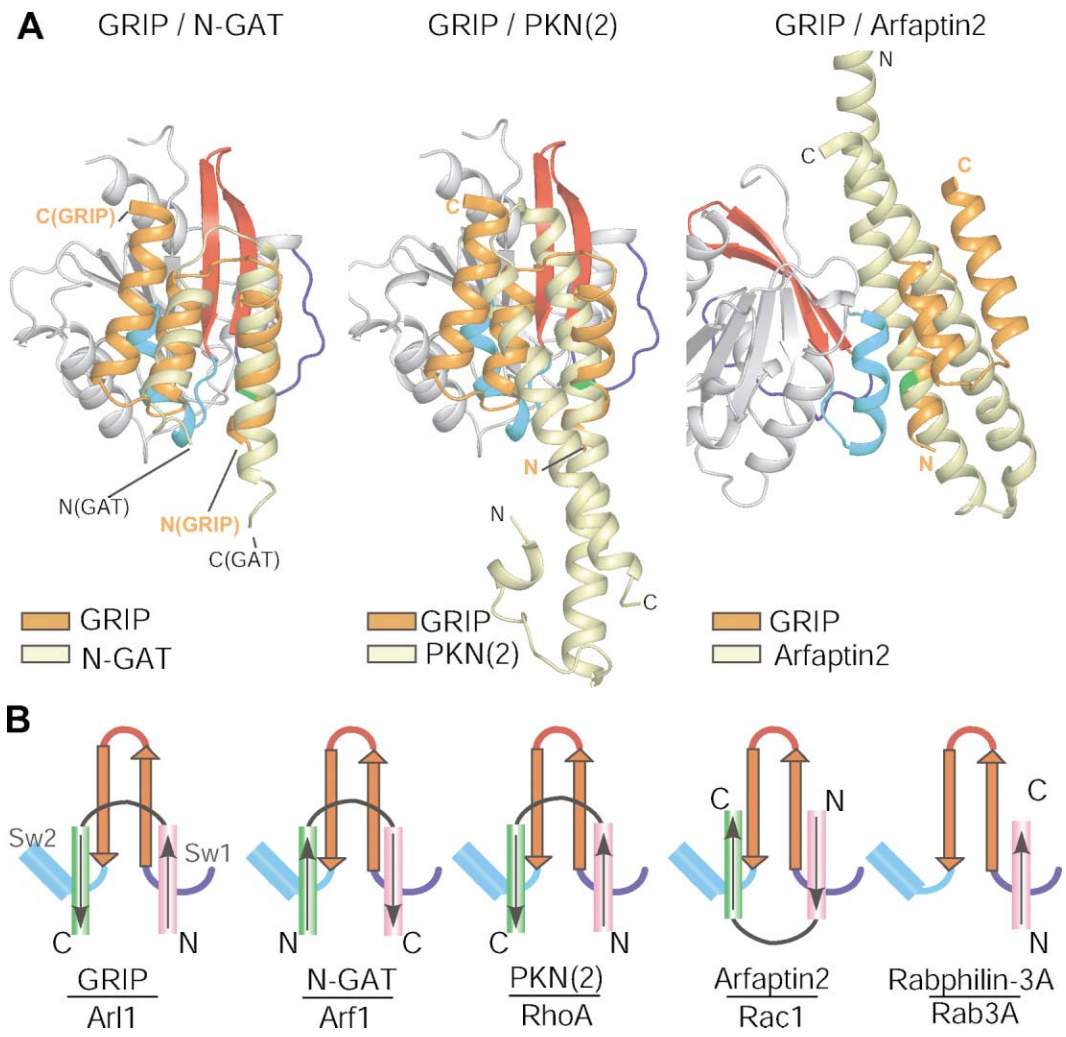

Figure 5. Comparison of the Arl1/GRIP Complex with Other GTPase/α-Helical Effector Complexes

(A) For comparison, the Arl1 from Arl1/GRIP complex was superimposed on the GTPase of each of the indicated GTPase/effector complexes. Both effectors are shown next to the ribbon diagram of Arl1 (gray), with switch 1 (blue), switch 2 (cyan), and interswitch (red). The GRIP domain is shown as an orange ribbon, while the N-GAT, PKN effector domain (contact 2), or Arfaptin2 is shown as tan ribbon. For simplicity, only a portion of Arfaptin2 is shown (helices A and B from molecule A).

(B) Schematic diagrams of helical pairs from different effectors interacting with switch 1 and switch 2 regions of their cognate GTPases.

GRIP domain was reduced by truncation at residue 2218, or mutation of residues Arg 2219–Leu 2224 to six alanines (Kjer-Nielsen et al., 1999b).

The tail region of the golgin-245 GRIP domain is not well resolved in the crystal structure, with helix α3 ending at residues 2220–2226 for three of the four domains in the asymmetric unit. However, in the case of the fourth GRIP domain, the tail lies against the surface of an adjacent Arl1-GTP/GRIP dimer, and although the side chains, including that of Trp 2223, cannot be resolved, it is clear that the backbone forms an α helix all the way to the C terminus at residue 2228. While this intermolecular interaction is almost certainly a consequence of the crystal environment, it indicates that the apparently unstructured C terminus has a propensity to form an α helix. A possible alternative inducer of a helical conformation is suggested by considering the likely orientation of the Arl1-GTP/GRIP complex on the lipid bilayer (Figure 6C). Insertion of the N-terminal myristoyl group and amphipathic helix of Arl1 into the lipid bilayer would orient the GRIP domain so that the C-terminal tail is adjacent to the bilayer surface. Formation of an α helix might then accompany insertion of the tryptophan and other hydrophobic residues into the lipid interfacial region (Figure 6C). Such an interaction would be analogous to the insertion of hydrophobic residues that accompanies the interaction of FYVE or PX domains with specific lipid head groups (Misra et al., 2001; Karathanassis et al., 2002; Stahelin et al., 2002). The interaction may serve to stabilize membrane attachment or to orient the domain to facilitate interaction with free Arl1-GTP diffusing in the plane of the bilayer.

Conclusions

The GRIP domain is responsible for targeting four golgins to the membranes of the *trans* Golgi. This targeting

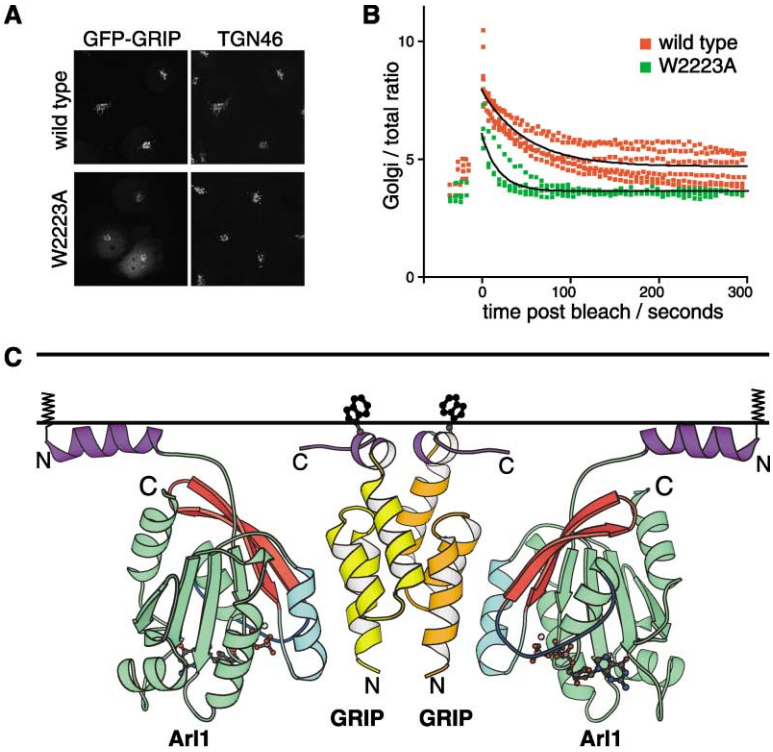

Figure 6. A Model of Arl1/GRIP Domain Dimers on the Golgi Membrane

(A) Confocal micrographs of GFP fusions to the C-terminal 82 residues of golgin-245 expressed in COS cells. The domain is either wild-type (Munro and Nichols, 1999) or has Trp 2223 mutated to alanine. After fixation and permeabilization, GFP and the Golgi marker TGN46 were localized by immunofluorescence.

(B) Equilibration between the cytoplasmic and Golgi-localized pools of the GFP-GRIP domains shown in (A). The non-Golgi pool was photobleached, and redistribution of the remaining protein was followed at 37°C using a Zeiss LSM510 microscope. The ratio between the Golgi and total signal over time is shown for the wild-type (n = 6) and the W2223A mutant (n = 4). For each construct the combined data sets were fitted to a single exponential to give half-lives of 34.8 s (95% confidence limits, 30.2–41.0) and 13.2 s (11.3–15.7), respectively.

(C) The structure of the Arl1/GRIP complex oriented with respect to the membrane in such a way that the N termini of Arl1 molecules and the C termini of GRIP molecules are facing the membrane. The N-terminal helix in Arl1 and the C-terminal helix in GRIP have been modeled and are colored purple. The N-terminal myristoyl group in each of the two Arl1 molecules can simultaneously bind to the same membrane. In addition, the Trp residue in the C-terminal region of each GRIP domain could penetrate in the interface region of the membrane, contributing to the stability of the complex on the Golgi membrane. The GTP binding sites on the two Arl1 molecules would be pointing away from the membrane, as would the rest of golgin-245. Although it cannot be excluded that Arl1 might be rotated by 90° so that the golgin lies along the membrane, the orientation shown here is the only one which allows for dyad symmetrical interactions of Arl1 and the GRIP domain with the lipid bilayer.

is mediated by binding of the GRIP domain to the GTPase Arl1, which is itself localized to the Golgi apparatus. In this paper we have shown that the GRIP domain forms a dimer that interacts bivalently with Arl1-GTP. In solution, the isolated domain is in a dimer-monomer equilibrium, but in the context of the golgins the extensive regions of coiled-coil in the rest of the proteins will presumably stabilize the dimer form. The interaction between Arl1-GTP and the GRIP domain is such that the membrane-bound GTPase will orient golgin-245 so that the C-terminal tail faces the lipid bilayer, and the rest of the molecule projects into the cytoplasm, either away from the Golgi membrane or along its surface. The interface formed between Arl1 and helices α1 and α2 of the GRIP domain is similar to that formed by several other Ras family GTPases with their effectors, suggesting that recognition of paired helices may be a widespread mechanism for effector binding. However, these other GTPases do not recognize their effectors with the dyad symmetric bivalency found in the Arl1-GTP/GRIP complex. Instead, this latter feature is strikingly reminiscent of the bivalent interaction between the endosomal tethering factor EEA1 and its lipid ligand PtdIns(3)P. In the case of EEA1, a C-terminal FYVE domain forms a dimer when stabilized by the parallel coiled-coils in the rest of the protein (Dumas et al., 2001). The resulting bivalent interaction with PtdIns(3)P is critical for ensuring the effective and accurate targeting of EEA1 to endosomes (Gillooly et al., 2000). Although both EEA1 and golgin-245 make dimeric association with membranes, the bivalent interaction of GRIP dimers with Arl1-GTP stands in distinction from the bivalent interaction of the FYVE domains with PtdIns(3)P. In EEA1, the affinity of each FYVE domain for PtdIns(3)P is fairly weak, and the presence of both domains in the dimer is necessary for translocation of EEA1 to membranes in cells. Given that a soluble, GTP-locked Arl1 forms a stable complex with GRIP that can be copurified in vitro, a single Arl1-GTP would probably be sufficient to cause GRIP homodimer translocation in cells. However, binding of a second Arl1-GTP by a GRIP homodimer at the membrane surface would increase the residence time of the complex on the membrane. Accuracy of membrane trafficking processes seems likely to be dependent on the cell being able to accurately specify both the location and the duration of targeting of the proteins that mediate docking and fusion (Munro, 2002). Bivalent interaction with organelle-specific GTPases or lipids may be one means by which this can be achieved.

Experimental Procedures

Protein Expression and Purification

Human Arl1 (residues 15–181, with the Q71L mutation and an N-terminal GST tag) was coexpressed with the nontagged GRIP domain from human golgin-245 (residues 2170–2228) using the polycistronic coexpression vector pOPCG. There are a number of splice variants of golgin-245, and all the work in this paper is based on isoform 4, Swissprot accession Q13439. SeMet-substituted protein for the crystallography was expressed in the *E. coli* methionine auxotroph B834(DE3) in M9 minimal medium supplemented with

amino acids, seleno-(L)-methionine, and vitamins as described previously (Karathanassis et al., 2002). Cells were grown to $OD_{600} = 1$ at 37°C and then induced with 0.3 mM IPTG at 17°C for 12 hr. Cells were lysed with a French press in buffer A (50 mM Tris-HCl [pH 7.5, 4°C], 100 mM NaCl, 5 mM $MgCl_2$, 10 mM β-mercaptoethanol, and 0.2 mM GTP). After ultracentrifugation, the complex was bound to glutathione-Sepharose (Amersham Biosciences), washed with buffer A, and cleaved on resin using 0.125 mg of tobacco etch virus protease (TEV) per 10 mg of complex for 12 hr at 4°C. After cleavage, Arl1 retained an N-terminal GSHM linker sequence. The complex was further purified by gel filtration on Superdex 75 16/60 equilibrated in buffer B (20 mM Tris [pH 7.5, 4°C], 100 mM NaCl, 1 mM $MgCl_2$, 5 mM DTT, and 10 μM GTP). The complex was concentrated to 11 mg/ml and snap frozen in liquid nitrogen.

Crystallization

Initial crystals were obtained at 17°C by vapor diffusion in sitting drops made by mixing 100 nl protein and 100 nl reservoir from crystallization screen Wizard I, condition 1 (Emerald BioStructures) in 96 well crystallization plates (Corning). Final conditions were optimized using hair seeding in hanging drops made by mixing 1 μl protein with 1 μl of reservoir solution consisting of 20% PEG 3350 and 0.2 M Tris-HCl (pH 8.5). After the crystals had reached their full size, the reservoir solution was exchanged for one containing 31% PEG 3350, and drops were incubated over this for approximately 2 days at 17°C. Crystals were frozen in cryoprotectant (31% PEG 3350, 0.2 M Tris-HCl [pH 8.5]).

Data Collection, Phasing, and Model Refinement

For data collection, crystals were frozen in a nitrogen gas stream, and data were collected at 100 K. Multiple anomalous dispersion (MAD) data sets were collected at ESRF beamline ID14-4 using an ADSC CCD detector. Prior to data collection, a fluorescence spectrum for the crystal was obtained, and three data sets were collected at wavelengths corresponding to the fluorescence peak, inflection, and a high energy remote. Table 1 lists statistics for data collection. Fifty putative Se sites were located using the program SnB (Turner et al., 1998; Weeks and Miller, 1999), and subsequent refinement with autoSHARP (de La Fortelle and Bricogne, 1997) resulted in 39 Se sites (Table 1). Solvent flattening was carried out with SOLOMON (Abrahams and Leslie, 1996), using a solvent content of 30.4% as optimized by SHARP. An initial model was built using Arp/warp (Perrakis et al., 1999) and refined by alternating rounds of refinement with REFMAC5 (CCP4, 1994) and manual rebuilding with the program O (Jones et al., 1991). Final statistics for the 1.7 Å resolution model are given in Table 1. There are no residues in the disallowed regions of the Ramachandran plot, and 95% of residues are in the most favored regions as defined by PROCHECK. Residues 2171–2220 are ordered for each of the GRIP domains in the asymmetric unit. The C-terminal residue ordered differs for each of the GRIP domains in the asymmetric unit: 2220, 2221, 2226, and 2228.

Coprecipitation Assays

His_6-tagged GRIP (golgin-245 residues 2170–2228) and MBP-tagged GRIP were produced in *E. coli* C41(DE3) either by coexpression from a polycistronic pOPC plasmid, with MBP-GRIP in the first cassette and His_6-GRIP in the second, or by expressing individually MBP-GRIP (from pOPTM plasmid, encoding an N-terminal MBP-tag) or His_6-GRIP (from pOPTH plasmid, encoding an N-terminal MetAlaHis_6Met-tag). Cells were grown in 2xTY/Amp to $OD_{600} = 1$ at 37°C, and then induced with 0.3 mM IPTG at 17°C for 12 hr. Cell pellets were lysed in PBS and bound to Ni-NTA (QIAGEN) resin, washed with PBS, and eluted with buffer containing 0.3 M imidazole, and aliquots were run on 20% Phast SDS gels (Amersham Biosciences).

Analytical Ultracentrifugation

Sedimentation equilibrium was performed on a Beckman Optima XLI ultracentrifuge using a Ti-60 rotor and interference and absorbance at 280 and 230 nm, at 10°C. His_6-GRIP domain from human golgin-245 expressed in *E. coli* C41(DE3) was purified by Ni^{2+}-affinity chromatography followed by gel filtration on a Superdex 75 16/60 column (Amersham Pharmacia) equilibrated in 20 mM Tris-HCl (pH 7.5, 4°C) and 100 mM NaCl. The protein was loaded into six-sector 12 mm path length cells at three different concentrations: 8 μM, 60 μM, and 220 μM. The samples were centrifuged until they reached equilibrium as judged by the changes in the subsequent scans. Speeds were 32,000, 38,000, and 45,000 rpm. Data were analyzed using UltraSpin software (www.mrc-cpe.cam.ac.uk).

Immunofluorescence

COS cells were transfected using FuGene (Roche), split onto glass slides, and fixed 30 hr post transfection with 4% paraformaldehyde, 0.1% glutaraldehyde. Cells were permeabilized with 0.5% (v/v) Triton X-100 in PBS, blocked with 20% (v/v) fetal calf serum/0.25% (v/v) Tween 20 in PBS, and probed with rabbit TGN46 antibodies (Prescott et al., 1997) and Alexa^{568} anti-rabbit antibodies (Molecular Probes). Images were obtained on a BioRad Radiance confocal microscope.

Acknowledgments

We thank Joanne McCarthy for assistance with data collection at ESRF beamline ID14-4, Ben Nichols for assistance with obtaining and analyzing photobleaching data, and Phil Evans, David Owen, and Katja Röper for critical reading of the manuscript.

Received: July 25, 2003
Revised: September 3, 2003
Accepted: September 5, 2003
Published: October 23, 2003

References

Abrahams, J.P., and Leslie, A.G.W. (1996). Methods used in the structure determination of bovine mitochondrial F1 ATPase. Acta Crystallogr. D *52*, 30–42.

Amor, J.C., Horton, J.R., Zhu, X., Wang, Y., Sullards, C., Ringe, D., Cheng, X., and Kahn, R.A. (2001). Structures of yeast ARF2 and ARL1: distinct roles for the N terminus in the structure and function of ARF family GTPases. J. Biol. Chem. *276*, 42477–42484.

Antonny, B., Beraud-Dufour, S., Chardin, P., and Chabre, M. (1997). N-terminal hydrophobic residues of the G protein ADP-ribosylation factor-1 insert into membrane phospholipids upon GDP to GTP exchange. Biochemistry *36*, 4675–4684.

Barr, F.A. (1999). A novel Rab6-interacting domain defines a family of Golgi-targeted coiled-coil proteins. Curr. Biol. *9*, 381–384.

Barr, F.A., and Short, B. (2003). Golgins in the structure and dynamics of the Golgi apparatus. Curr. Opin. Cell Biol. *15*, 405–413.

Bhamidipati, A., Lewis, S.A., and Cowan, N.J. (2000). ADP ribosylation factor-like protein 2 (Arl2) regulates the interaction of tubulin-folding cofactor D with native tubulin. J. Cell Biol. *149*, 1087–1096.

Bi, X., Corpina, R.A., and Goldberg, J. (2002). Structure of the Sec23/24-Sar1 pre-budding complex of the COPII vesicle coat. Nature *419*, 271–277.

Bonangelino, C.J., Chavez, E.M., and Bonifacino, J.S. (2002). Genomic screen for vacuolar protein sorting genes in *Saccharomyces cerevisiae*. Mol. Biol. Cell *13*, 2486–2501.

CCP4 (Collaborative Computing Project Number 4) (1994). A suite of programs for protein crystallography. Acta Crystallogr. D *50*, 760–763.

Chavrier, P., and Goud, B. (1999). The role of ARF and Rab GTPases in membrane transport. Curr. Opin. Cell Biol. *11*, 466–475.

Clark, J., Moore, L., Krasinskas, A., Way, J., Battey, J., Tamkun, J., and Kahn, R.A. (1993). Selective amplification of additional members of the ADP-ribosylation factor (ARF) family: cloning of additional human and *Drosophila* ARF-like genes. Proc. Natl. Acad. Sci. USA *90*, 8952–8956.

Collins, B.M., Watson, P.J., and Owen, D.J. (2003). The structure of the GGA1-GAT domain reveals the molecular basis for ARF binding and membrane association of GGAs. Dev. Cell *4*, 321–332.

de La Fortelle, E., and Bricogne, G. (1997). Maximum-likelihood heavy-atom parameter refinement for multiple isomorphous re-

placement and multiwavelength anomalous diffraction methods. Methods Enzymol. *276*, 472–494.

Donaldson, J.G., and Jackson, C.L. (2000). Regulators and effectors of the ARF GTPases. Curr. Opin. Cell Biol. *12*, 475–482.

Dumas, J.J., Merithew, E., Sudharshan, E., Rajamani, D., Hayes, S., Lawe, D., Corvera, S., and Lambright, D.G. (2001). Multivalent endosome targeting by homodimeric EEA1. Mol. Cell *8*, 947–958.

Erlich, R., Gleeson, P.A., Campbell, P., Dietzsch, E., and Toh, B.H. (1996). Molecular characterization of *trans*-Golgi p230. A human peripheral membrane protein encoded by a gene on chromosome 6p12–22 contains extensive coiled-coil α-helical domains and a granin motif. J. Biol. Chem. *271*, 8328–8337.

Fritzler, M.J., Lung, C.C., Hamel, J.C., Griffith, K.J., and Chan, E.K. (1995). Molecular characterization of Golgin-245, a novel Golgi complex protein containing a granin signature. J. Biol. Chem. *270*, 31262–31268.

Gangi Setty, S.R., Shin, M.E., Yoshino, A., Marks, M.S., and Burd, C.G. (2003). Golgi recruitment of GRIP domain proteins by Arf-like GTPase 1 (Arl1p) is regulated by the Arf-like GTPase 3 (Arl3p). Curr. Biol. *13*, 401–404.

Goldberg, J. (1998). Structural basis for activation of ARF GTPase: mechanisms of guanine nucleotide exchange and GTP-myristoyl switching. Cell *95*, 237–248.

Gillingham, A.K., and Munro, S. (2003). Long coiled-coil proteins and membrane traffic. Biochim. Biophys. Acta *1641*, 71–85.

Gillooly, D.J., Morrow, I.C., Lindsay, M., Gould, R., Bryant, N.J., Gaullier, J.M., Parton, R.G., and Stenmark, H. (2000). Localization of phosphatidylinositol 3-phosphate in yeast and mammalian cells. EMBO J. *19*, 4577–4588.

Hanzal-Bayer, M., Renault, L., Roversi, P., Wittinghofer, A., and Hillig, R.C. (2002). The complex of Arl2-GTP and PDE delta: from structure to function. EMBO J. *21*, 2095–2106.

Jones, T.A., Zou, J.-Y., Cowan, S.W., and Kjeldgaard, M. (1991). Improved methods for building protein models in electron density maps and the location of errors in these models. Acta Crystallogr. A *47*, 110–119.

Karathanassis, D., Stahelin, R.V., Bravo, J., Perisic, O., Pacold, C.M., Cho, W., and Williams, R.L. (2002). Binding of the PX domain of $p47^{phox}$ to phosphatidylinositol 3,4-bisphosphate and phosphatidic acid is masked by an intramolecular interaction. EMBO J. *21*, 5057–5068.

Kjer-Nielsen, L., Teasdale, R.D., van Vliet, C., and Gleeson, P.A. (1999a). A novel Golgi-localisation domain shared by a class of coiled- coil peripheral membrane proteins. Curr. Biol. *9*, 385–388.

Kjer-Nielsen, L., van Vliet, C., Erlich, R., Toh, B.H., and Gleeson, P.A. (1999b). The Golgi-targeting sequence of the peripheral membrane protein p230. J. Cell Sci. *112*, 1645–1654.

Kooy, J., Toh, B.H., Pettitt, J.M., Erlich, R., and Gleeson, P.A. (1992). Human autoantibodies as reagents to conserved Golgi components. Characterization of a peripheral, 230 kDa compartment-specific Golgi protein. J. Biol. Chem. *267*, 20255–20263.

Krauss, M., Kinuta, M., Wenk, M.R., De Camilli, P., Takei, K., and Haucke, V. (2003). ARF6 stimulates clathrin/AP-2 recruitment to synaptic membranes by activating phosphatidylinositol phosphate kinase type Iγ. J. Cell Biol. *162*, 113–124.

Lee, F.J.S., Huang, C.F., Yu, W.L., Buu, L.M., Lin, C.Y., Huang, M.C., Moss, J., and Vaughan, M. (1997). Characterization of an ADP-ribosylation factor-like 1 protein in *Saccharomyces cerevisiae*. J. Biol. Chem. *272*, 30998–31005.

Li, B., and Warner, J.R. (1996). Mutation of the Rab6 homolog of *Saccharomyces cerevisiae*, *YPT6*, inhibits both early Golgi function and ribosome biosynthesis. J. Biol. Chem. *271*, 16813–16819.

Lowe, S.L., Wong, S.H., and Hong, W. (1996). The mammalian ARF-like protein 1 (Arl1) is associated with the Golgi complex. J. Cell Sci. *109*, 209–220.

Lu, L., and Hong, W. (2003). Interaction of Arl1-GTP with GRIP domains recruits autoantigens Golgin-97 and Golgin-245/p230 onto the Golgi. Mol. Biol. Cell *14*, 3767–3781.

Lu, L., Horstmann, H., Ng, C., and Hong, W. (2001). Regulation of Golgi structure and function by ARF-like protein 1 (Arl1). J. Cell Sci. *114*, 4543–4555.

Luke, M.R., Kjer-Nielsen, L., Brown, D.L., Stow, J.L., and Gleeson, P.A. (2003). GRIP domain-mediated targeting of two new coiled-coil proteins, GCC88 and GCC185, to subcompartments of the trans-Golgi network. J. Biol. Chem. *278*, 4216–4226.

Maesaki, R., Ihara, K., Shimizu, T., Kuroda, S., Kaibuchi, K., and Hakoshima, T. (1999). The structural basis of Rho effector recognition revealed by the crystal structure of human RhoA complexed with the effector domain of PKN/PRK1. Mol. Cell *4*, 793–803.

McConville, M.J., Ilgoutz, S.C., Teasdale, R.D., Foth, B.J., Matthews, A., Mullin, K.A., and Gleeson, P.A. (2002). Targeting of the GRIP domain to the trans-Golgi network is conserved from protists to animals. Eur. J. Cell Biol. *81*, 485–495.

Misra, S., Miller, G.J., and Hurley, J.H. (2001). Recognizing phosphatidylinositol 3-phosphate. Cell *107*, 559–562.

Mueller, A.G., Moser, M., Kluge, R., Leder, S., Blum, M., Buttner, R., Joost, H.G., and Schurmann, A. (2002). Embryonic lethality caused by apoptosis during gastrulation in mice lacking the gene of the ADP-ribosylation factor-related protein 1. Mol. Cell. Biol. *22*, 1488–1494.

Munro, S. (2002). Organelle identity and the targeting of peripheral membrane proteins. Curr. Opin. Cell Biol. *14*, 506–514.

Munro, S., and Nichols, B.J. (1999). The GRIP domain: a novel Golgi-targeting domain found in several coiled-coil proteins. Curr. Biol. *9*, 377–380.

Nassar, M., Horn, G., Herrmann, C., Scherer, A., McCormick, F., and Wittinghofer, A. (1995). The 2.2 Å crystal structure of the Ras binding domain of the serine/threonine kinase c-Raf1 in complex with Rap1A and a GTP analog. Nature *375*, 554–560.

Niedergang, F., Colucci-Guyon, E., Dubois, T., Raposo, G., and Chavrier, P. (2003). ADP ribosylation factor 6 is activated and controls membrane delivery during phagocytosis in macrophages. J. Cell Biol. *161*, 1143–1150.

Ostermeier, C., and Brunger, A.T. (1999). Structural basis of Rab effector specificity: crystal structure of the small G protein Rab3A complexed with the effector domain of rabphilin-3A. Cell *96*, 363–374.

Pacold, M.E., Suire, S., Perisic, O., Lara-Gonzalez, S., Davis, C.T., Walker, E.H., Hawkins, P.T., Stephens, L., Eccleston, J.F., and Williams, R.L. (2000). Crystal structure and functional analysis of Ras binding to its effector phosphoinositide 3-kinase γ. Cell *103*, 931–943.

Panic, B., Whyte, J.R., and Munro, S. (2003). The ARF-like GTPases Arl1p and Arl3p act in a pathway that interacts with vesicle-tethering factors at the Golgi apparatus. Curr. Biol. *13*, 405–410.

Pasqualato, S., Menetrey, J., Franco, M., and Cherfils, J. (2001). The structural GDP/GTP cycle of human Arf6. EMBO Rep. *2*, 234–238.

Pasqualato, S., Renault, L., and Cherfils, J. (2002). Arf, Arl, Arp and Sar proteins: a family of GTP binding proteins with a structural device for 'front-back' communication. EMBO Rep. *3*, 1035–1041.

Perrakis, A., Morris, R., and Lamzin, V.S. (1999). Automated protein model building combined with iterative structure refinement. Nat. Struct. Biol. *6*, 458–463.

Pfeffer, S.R. (1999). Transport-vesicle targeting: tethers before SNAREs. Nat. Cell Biol. *1*, E17–E22.

Prescott, A.R., Lucocq, J.M., James, J., Lister, J.M., and Ponnambalam, S. (1997). Distinct compartmentalization of TGN46 and β1,4-galactosyltransferase in HeLa cells. Eur. J. Cell Biol. *72*, 238–246.

Shiba, T., Kawasaki, M., Takatsu, H., Nogi, T., Matsugaki, N., Igarashi, N., Suzuki, M., Kato, R., Nakayama, K., and Wakatsuki, S. (2003). Molecular mechanism of membrane recruitment of GGA by ARF in lysosomal protein transport. Nat. Struct. Biol. *10*, 386–393.

Shorter, J., and Warren, G. (2002). Golgi architecture and inheritance. Annu. Rev. Cell Dev. Biol. *18*, 379–420.

Stahelin, R.V., Long, F., Diraviyam, K., Bruzik, K.S., Murray, D., and Cho, W. (2002). Phosphatidylinositol-3-phosphate induces the membrane penetration of the FYVE domains of Vps27p and Hrs. J. Biol. Chem. *277*, 26379–26388.

Takai, Y., Sasaki, T., and Matozaki, T. (2001). Small GTP binding proteins. Physiol. Rev. *81*, 153–208.

Tamkun, J.W., Kahn, R.A., Kissinger, M., Brizuela, B.J., Rulka, C., Scott, M.P., and Kennison, J.A. (1991). The arflike gene encodes an essential GTP binding protein in *Drosophila*. Proc. Natl. Acad. Sci. USA *88*, 3120–3124.

Tarricone, C., Xiao, B., Justin, N., Walker, P.A., Rittinger, K., Gamblin, S.J., and Smerdon, S.J. (2001). The structural basis of Arfaptin-mediated cross-talk between Rac and Arf signaling pathways. Nature *411*, 215–219.

Tsukada, M., Will, E., and Gallwitz, D. (1999). Structural and functional analysis of a novel coiled-coil protein involved in Ypt6 GTPase-regulated protein transport in yeast. Mol. Biol. Cell *10*, 63–75.

Turner, M.A., Yuan, C.-S., Borchardt, R.T., Hershfield, M.S., Smith, G.D., and Howell, L.L. (1998). Structure determination of selenomethionyl S-adenosylhomocysteine hydrolase using data at a single wavelength. Nat. Struct. Biol. *5*, 369–376.

Van Valkenburgh, H., Shern, J.F., Sharer, J.D., Zhu, X., and Kahn, R.A. (2001). ADP-ribosylation factors (ARFs) and ARF-like 1 (ARL1) have both specific and shared effectors: characterizing ARL1 binding proteins. J. Biol. Chem. *276*, 22826–22837.

Vetter, I.R., and Wittinghofer, A. (2001). The guanine nucleotide binding switch in three dimensions. Science *294*, 1299–1304.

Weeks, C.M., and Miller, R. (1999). The design and implementation of SnB v2.0. J. Appl. Crystallogr. *32*, 120–124.

Accession Numbers

The coordinates of the Arl1-GTP/GRIP domain complex have been deposited in the Protein Data Bank under the ID code 1UPT.